

## Photolithographic Production of Glass Sample Holders for Improved Sensitivity and Resolution in ESR Microscopy

R. Halevy, Y. Talmon, and A. Blank

Schulich Faculty of Chemistry, Technion – Israel Institute of Technology, Haifa, Israel

Received July 31, 2006; revised August 31, 2006

**Abstract.** Electron spin resonance microscopy (ESRM) is an imaging method aiming at the observation of stable free radicals in small samples with a spatial resolution of about 1 micrometer. One of the challenges associated with the use of ESRM in conjunction with small biological samples (e.g., single cells) is containing these samples in a manner that will minimize the effect on the quality factor of the resonator but yet enable easy handling and simultaneous optical and ESR observation. Here we present a new type of flat samples that provide an adequate answer to this challenge. The samples are made of thin glass coverslips, manufactured by photolithography techniques. Details of the manufacturing process as well as the expected improvements in sensitivity and resolution are provided.

### 1 Introduction

Electron spin resonance (ESR) microscopy is an emerging imaging technique with many possible biological and medical applications [1]. Traditionally, most ESR imaging efforts have been directed towards studies of large biological subjects *in vivo*, with relatively low resolution (ca. 1–10 mm), to identify the radical and oxygen concentrations (by its effect on the radical line width) [2, 3]. ESR microscopy (ESRM) is complementary to the more common *in vivo* imaging approach. It is based on scaling down the size of the imaging probe employed and thereby measuring small microscopic samples by the use of miniature resonators and gradient coils [1, 4, 5]. The scaling down, along with the use of relatively high microwave frequencies (10–60 GHz vs. about 0.2–1 GHz employed in *in vivo* ESR) enables one to significantly improve upon both spin sensitivity and image resolution (down to about 1  $\mu\text{m}$  resolution).

ESRM can be applied to a variety of scientific issues of interest such as the imaging of live cells with subcellular resolution for biophysical applications [1], observation of chemical reactions and degradation processes in small pallets [6], controlled drug release from microspheres [7], and the imaging of radiation-in-

duced defects in semiconductors [8]. In many of these applications, ESRM could provide information complementary to that obtained by more common techniques such as fluorescence and atomic force microscopy. For example, ESR can be used to accurately map  $O_2$  concentration [2, 9], reveal chemical specific information about reactive oxygen and nitrogen species [10–12], measure and image microviscosity [13], pH [14], and redox state [15]. All these parameters of interest were already measured with conventional “spectroscopic” ESR, as well as with large-scale ESR imaging machines and could therefore be acquired by ESRM measurements.

As mentioned above, one of the main features of ESRM is the use of a tiny resonator for improved sensitivity and resolution. We have found it most useful to construct the resonator from a single crystal of high-permittivity material (e.g.,  $SrTiO_3$ , or  $TiO_2$ ) and to produce it in the shape of a ring [1, 4, 16, 17]. The compactness of the resonator increases the density of the electromagnetic energy stored at the sample position. The magnetic and electric fields of typical single-ring and double-stacked-rings resonators are shown in Figs. 1 and 2, respectively. Both configurations show good separation between the electric and magnetic components of the microwave field. The electric field is mostly confined to the dielectric rings, whereas the magnetic component is mainly around the central axis of the resonators. Such field distribution makes it possible to place a tubelike sample in the center of the resonator, where the electric field is minimal and the magnetic field is at maximum, thus improving the sensitivity and image resolution [7, 17].

The common tubelike sample containers, which are optimized for the measurements of homogenous samples, are far from optimal when microscopic imaging of subjects such as live cells or tissue extracts is needed. This is especially true when considering the small dimensions of the ESRM ring resonators described here, which can only accommodate tubes with an outer diameter that is smaller than about 1 mm. Placing microscopic samples of interest inside such a thin tube is very difficult and calls for nonstandard and cumbersome sample

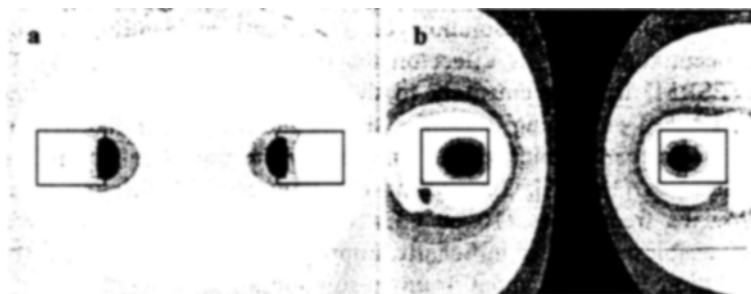


**Fig. 1.** a Cross section of the calculated microwave magnetic fields of a typical single-ring resonator. The resonator structure cross section is marked by the two black rectangles. Calculations were performed by CST (computer simulation technology) microwave studio. b The same as a but for the microwave electric fields.

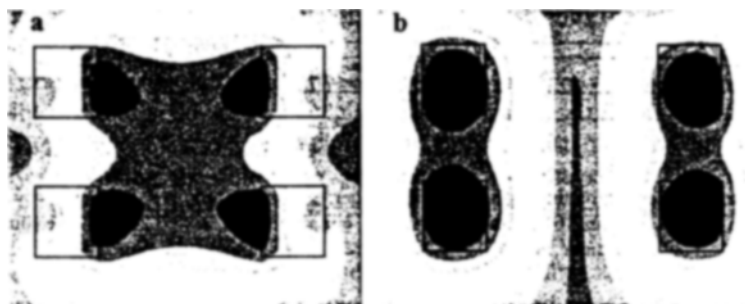


**Fig. 2.** **a** Cross section of the calculated microwave magnetic fields of a typical double-stacked-rings resonator. The resonator structure cross section is marked by the two black rectangles. Calculations were performed by CST microwave studio. **b** The same as **a** but for the microwave electric fields.

preparation procedures. Furthermore, one would like to observe the sample also by a conventional optical microscope while it is being measured by the ESRM system. This requirement is also very difficult to accommodate when employing tubelike sample holders. It can be concluded that these limitations warrant the design and fabrication of new types of sample holders, which are better optimized for ESRM applications. Simple preparation of biological samples and supporting simultaneous ESR and optical imaging are not the only issues to be considered. For the new sample holders two additional factors must also be taken into considerations. First, since biological samples are aqueous in nature and therefore tend to strongly absorb the incident microwave energy [18], the new holders must position the sample in areas of low electric field, in order to minimize the dielectric losses and sample microwave heating. Second, the design of the sample holders should carefully optimize important parameters that affect the signal-to-noise ratio (SNR) of the ESR signal such as the quality factor ( $Q$ ) of the resonator plus sample, and the filling factor of the sample in the resonator.

In order to overcome the difficulties associated with the tubelike sample containers and to properly address the challenges raised above, an alternative approach for holding the sample during the measurement was considered. The main idea is to base the new design on flat sample holders, similar to the ones shown in Figs. 3 and 4. Flat sample holders are commonly used in millimeter-wave ESR measurements [19, 20] and recently this approach proved itself

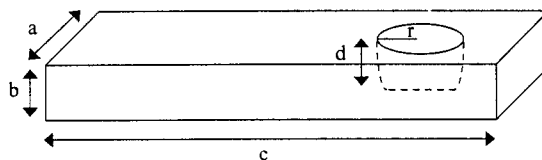


**Fig. 3.** Schematic drawing of the first type of the flat glass sample holder:  $a = 3.7$  mm,  $b = 0.2$  mm,  $c = 21.9$  mm,  $d = 0.1$  mm and the radius  $r$  is 0.5 mm.

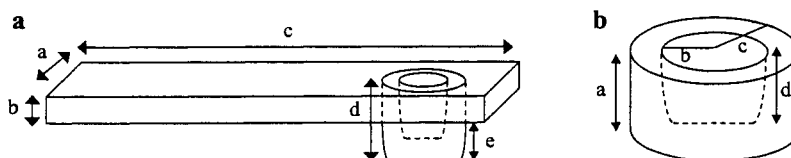


**Fig. 4.** Schematic drawing of the cuplike sample holder: **a**  $a = 3.7$  mm,  $b = 0.17$  mm,  $c = 21.9$  mm,  $d = 0.2$  mm,  $e = 0.03$  mm. **b** “Zoom-in” on the cup structure:  $a = 0.2$  mm, the inner radius  $b = 0.3$  mm, the outer radius  $c = 0.35$  mm, and the depth of the cup  $d = 0.1$  mm.

in a 16 GHz ESRM study of the controlled drug release by microspheres [7]. However, up to now both high-field ESR and ESRM employed very crude and simple low-precision processes to fabricate these sample holders, such as creating patterns with paraffin wax and subsequently etching the glass with hydrofluoric acid (HF). These “manual” preparation methods are not applicable for tiny millimeter-sized resonators and cannot be of common practical use. Here we present a more precise manufacturing process of flat glass sample holders, prepared by means of the well-known photolithography technique. Photolithography offers the capability to produce patterns with high precision and resolution on the glass surface and was found useful for dealing with the present sample holder problem. In Sect. 2 we shall detail the preparation method of the sample holders and in Sect. 3 we shall describe the holders’ geometry and discuss their implications upon the quality and filling factors and upon the SNR.

## 2 Experimental

Photolithography is a well developed technique used both for research and in commercial production. Nevertheless, despite the significant advance and the wide availability of photolithography technology, there are still several production tasks that require nontrivial processing in order to obtain the desired results. One such issue is the deep etching of glass slides employing conventional photoresist masking. Although there are several recent publications that deal with this issue [21–23], there is still no “fail-proof” procedure that works well with common glass and provides robust results under the ever changing physical conditions (i.e., temperature, humidity) of clean-room facilities. The most problematic step in deep etching of glass with photoresist masking is the etching itself, which often causes the photoresist to peel off the glass prior to the end of the process. One way of overcoming this problem is to conduct the etching step after applying chrome and/or gold masking in addition to the photoresist [24]. However, such procedure significantly increases the complexity of the entire process and therefore it is not suitable for the production of many sample holders, as needed for common ESRM applications. To avoid photoresist peeling-off during the etching process, we took a combined approach which (a) uses an “easy-to-etch” glass;

- (b) maximizes the adhesion quality of the photoresist onto the glass surface; and
- (c) employs relatively weak etchant.

The first issue was addressed by employing a relatively low-quality and non-chemically resistant soda-lime cover glass with a thickness of 200  $\mu\text{m}$  (from AVX, Israel). The aspect of strong adhesion of the photoresist onto the glass was obtained by employing the following procedure. First, the slides were thoroughly cleaned to remove all organic particles and metallic contamination. The cleaning solution consisted of a mixture of  $\text{H}_2\text{SO}_4$  (98%) and  $\text{H}_2\text{O}_2$  (30%) (2:1) and the glass slides were kept over night in the solution. Following the cleaning, the slides were rinsed with deionized water, spin dried and baked on a hot plate at 300  $^\circ\text{C}$  for 20 min to remove any residual water molecules. In the next step, the slide surface was treated by hexamethyl disilazane (HMDS), to further promote the adhesion of the photoresist, and then baked in an oven at 90  $^\circ\text{C}$  for 10 min. Slides were then spin coated with AZ5214E photoresist (Clariant Corporation, USA) for 60 s at 4000 rpm. Following the coating, slides were prebaked in an oven at 90  $^\circ\text{C}$  for 10 min, in order to accelerate the diffusion of the solvent out of the resist film. The final thickness of AZ5214E after spin coating was measured to be about 1.4  $\mu\text{m}$ . The slides were then exposed to a UV light source through a photomask at *g*-line wavelength for 4 s with an intensity of 10  $\text{mW}\cdot\text{cm}^{-2}$ . Photoresist development was carried out with a standard developer (tetramethylammonium hydroxide (TMAH) (1:10); Mallinckrodt Baker Inc, Phillipsburg, NJ, USA) for 30 s, followed by rinsing with deionized water and spin drying. Next the photoresist is further hardened by a 1 min UV light flood exposure and postbaked in an oven at 120  $^\circ\text{C}$  for 2 h. In order to prevent unwanted etching of the back side of the slides, the glass slides are then spin coated with another type of photoresist (1818 from Shipley, UK) for 60 s at 4000 rpm and inserted into the oven for an additional postbaking period of 2 h at 120  $^\circ\text{C}$ . Prior to the etching step the slides were treated by oxygen plasma descum for 1 min in order to remove any excess undeveloped HMDS and to accelerate the etching. The etching step itself was carried out with a relatively mild acid, namely, fluorosillicic acid (35% technical grade, Sigma) at 50  $^\circ\text{C}$  for 2 h. The etching rate of the glass under these conditions was found to be about 0.7  $\mu\text{m}$  per minute. Finally, the photoresist was removed and slides were cleaned with acetone.

In the case of the cuplike shaped slides (Fig. 4), production is carried out in two steps. The first step produces the patterns on the upper side of the glass, in an identical manner to the method described above (with a slightly different mask).

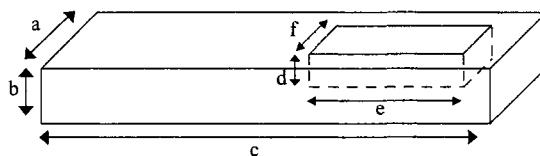


Fig. 5. Schematic drawing of the cover glass slide:  $a = 3.7$  mm,  $b = 0.2$  mm,  $c = 21.9$  mm,  $d = 0.05$  mm,  $e = 3.5$  mm,  $f = 2.1$  mm.

The second step is similar to the first one, but here the mask of the back side must be aligned, prior to photoexposure, with respect to the patterns produced on the upper side of the glass. This is done by the use of a mask aligner (MA6 Contact Mask aligner, BSA system UV 400; Karl Suss America Inc., Waterbury Center, Vermont, USA). Yet another type of glass slide that is produced to complete the sample container is a cover slide (Fig. 5). The cover glass piece, which can be bonded with an appropriate adhesive to the bottom glass, is required for a complete isolation of the sample from the outside, in case it needs to be examined under vacuum or controlled atmospheric condition, and/or to avoid sample dehydration.

### 3 Results and Discussion

As noted above, two main types of sample holders were produced, with the same matching cover glass for both types. The first type of sample holder has circular shape and its total thickness, with the cover glass, enables it to fit into the space between the rings of the double-stacked resonator configuration (Figs. 2 and 3). The second type is a cuplike sample holder that can be inserted right into the circular single-ring resonator (Figs. 1 and 4). While the first type of sample holder is easier to produce, the second type offers better sensitivity and consequently better image resolution, as shall be shown below.

Let us now analyze the calculated microwave electric and magnetic field distribution (shown in Figs. 1 and 2) in terms of the corresponding filling factor of the sample inside the resonators and the quality factor of the resonators. For the double-stacked resonator, which was employed in previous ESRM work [17], the calculated filling factor of a cylindrical sample 0.2 mm in diameter and 0.2 mm in height, located in the center of the resonator, was found to be 0.0057. This value “translates” to an effective volume of  $V_c = 1.10 \text{ mm}^3$ , where the term “effective volume” refers to the ratio between this small (pointlike) sample volume and its filling factor [1]. The smaller the effective volume, the larger the SNR of a standard small-sized sample would be. (In ESRM the “standard small-size sample” would typically be a single image voxel.) The calculated quality factor of the double-stacked resonator, containing a sample made of standard saline solution (permittivity  $\epsilon = 80$  and conductivity  $\sigma = 0.8 \text{ S/m}$ ) that fills in the entire etched circular hole of the sample holder (Fig. 3) was found to be 280. This value is a bit small compared with the  $Q$  of the empty resonator, calculated to be 2566. Nevertheless, it is still high enough to support the ESR measurements in terms of efficient frequency locking on the resonator resonance, and reasonable SNR. For the single-ring resonator, similar calculations resulted in a small sample (0.2 mm diameter, 0.2 mm height) filling factor of 0.01, which implies an effective volume of  $V_c = 0.0063 \text{ mm}^3/0.01 = 0.63 \text{ mm}^3$ . The effects on  $Q$  were similar to the ones calculated for the double-stacked resonator.

Let us analyze the meaning of  $V_c$  and  $Q$  that were calculated above in terms of the SNR. For pulsed ESR the single-shot SNR is given by [1, 5]:

$$\text{SNR}_{\text{pulse}} \approx \frac{\sqrt{2} \sqrt{2\mu_0} M V_v \omega_0}{16 \sqrt{V_c} \sqrt{k_b T \Delta f}} \sqrt{\frac{Q_u}{\omega_0}}, \quad (1)$$

where  $\mu_0$  is the free space permeability,  $M$  is the sample magnetization,  $V_v$  is the volume of the sample of interest (a single voxel),  $k_b$  is the Boltzmann constant,  $T$  is the temperature,  $\Delta f$  is the bandwidth of acquisition, and  $\omega_0$  is the angular microwave frequency. Equation (1) enables one to realize the importance of the new sample holders in a quantitative manner. First of all, by localizing the sample in the center of the resonator (in both configurations), one can minimize the dielectric losses. As a consequence, the value of  $Q$  (with a lossy sample) would typically be about 200–400 (depending on the exact sample size). ( $Q$  may be even larger if only small samples of  $<100 \mu\text{m}$  are considered, which can be realized by fabrication of smaller sample containers.) Without exact localization of the sample in the center, flat samples in single or double-stacked resonator would cause the value of  $Q$  to be as low as 30–60. Such low value makes it difficult to lock on the resonance frequency of the resonator and implies a reduction in SNR by a factor of about 3–4 compared with the localized case (achieved by the photolithographic process). In addition to the effects on  $Q$ , the cuplike sample holder (Fig. 4) enables one to employ a flat sample holder, with all its advantages (accessibility of samples, optical imaging capability), in conjunction with single-ring resonator. The use of a single-ring resonator, which has an effective volume,  $V_c$ , that is almost a factor of 2 smaller than that of the double-stacked resonator, results in an additional improvement in the SNR by a factor of  $\sqrt{2}$  (Eq. (1)). Therefore, the combined increase in SNR, when comparing the new sample holders with those created without accurate photolithography processing, mounts up to a factor of about 5–6, which implies an improvement by a factor of about 1.8 in the three-dimensional image resolution, or reduction in acquisition time by a factor of about 30, when keeping image resolution the same.

#### 4 Summary and Conclusions

This study presents the application of photolithography for the development of micro glass sample holders used in ESR microimaging. The high resolution of the patterns created on the sample holders enables one to overcome many of the difficulties associated with the use of conventional ESR sample tubes (e.g., handling of small samples and optical accessibility) and also significantly improves the SNR. Thus, the new approach would enable one to examine small objects by both optical and ESR microscopy at the same time, where the sample contains a minimum amount of water, leading to improved quality and filling factors. This is a key issue that would significantly improve the capabilities and qualities of high-frequency ESR microimaging. The sample holders are easy to produce with high precision, which is important if one wishes to enable wide availability of ESR microimaging as a state-of-art tool in bioscience and biotechnology.

### Acknowledgments

This work was partially supported by grants 169/05 and 1143/05 by the Israeli Science Foundation, and by a grant from the the Russell Berrie Nanotechnology Institute at the Technion.

### References

1. Blank A., Dunnam C.R., Borbat P.P., Freed J.H.: *J. Magn. Reson.* **165**, 116–127 (2003)
2. Liu K.J., Grinstaff M.W., Jiang J., Suslick K.S., Swartz H.M., Wang W.: *Biophys. J.* **67**, 896–901 (1994)
3. Halpern H.J., Peric M., Nguyen T.D., Spencer D.P.: *J. Magn. Reson.* **90**, 40–47 (1990)
4. Blank A., Dunnam C.R., Borbat P.P., Freed J.H.: *Rev. Sci. Instrum.* **75**, 3050–3061 (2004)
5. Blank A., Dunnam C.R., Borbat P.P., Freed J.H.: *Appl. Phys. Lett.* **85**, 5430–5432 (2004)
6. Xiang Z., Xu Y.: *Appl. Magn. Reson.* **12**, 69–79 (1997)
7. Blank A., Freed J.H., Naraharisetti P.K., Wang C.H.: *J. Control. Release* **111**, 174–184 (2006)
8. Ikeya M.: *Annu. Rev. Mater. Sci.* **21**, 45–63 (1991)
9. Swartz H.M., Clarkson R.B.: *Phys. Med. Biol.* **43**, 1957–1975 (1998)
10. Murrant C.L., Reid M.B.: *Microsc. Res. Tech.* **55**, 236–248 (2001)
11. Pandian R., Dang V., Manoharan P.T., Zweier J.L., Kuppusamy P.: *J. Magn. Reson.* **181**, 154–161 (2006)
12. Rizzi C., Samouilov A., Kutala V.K., Parinandi N.L., Zweier J.L., Kuppusamy P.: *Free Radic. Biol. Med.* **35**, 1608–1618 (2003)
13. Halpern H.J., Chandramouli G.V.R., Barth E.D., Yu C., Peric M., Grdina D.J., Teicher B.A.: *Cancer Res.* **59**, 5836–5841 (1999)
14. Gallez B., Mader K., Swartz H.M.: *Magn. Reson. Med.* **36**, 694–697 (1996)
15. Kuppusamy P., Krishna M.C.: *Curr. Top. Biophys.* **26**, 29–34 (2002)
16. Blank A., Stavitski E., Levanon H., Gubaydullin F.: *Rev. Sci. Instrum.* **74**, 2853–2859 (2003)
17. Jaworski M., Sienkiewicz A., Scholes C.P.: *J. Magn. Reson.* **124**, 87–96 (1997)
18. Nesmelov Y.E., Gopinath A., Thomas D.D.: *J. Magn. Reson.* **167**, 138–146 (2004)
19. Barnes J.P., Freed J.H.: *Rev. Sci. Instrum.* **68**, 2838–2846 (1997)
20. Smith G.M., Lesurf J.C.G., Mitchell R.H., Riedi P.C.: *Rev. Sci. Instrum.* **69**, 3924–3937 (1998)
21. Grosse A., Grewe M., Fouckhardt H.: *J. Micromech. Microeng.* **11**, 257–262 (2001)
22. Bien D.C.S., Rainey P.V., Mitchell S.J.N., Gamble H.S.: *J. Micromech. Microeng.* **13**, 34–40 (2003)
23. Bu M., Melvin T., Ensell G.J., Wilkinson J.S., Evans A.G.R.: *Sensors Actuators A* **115**, 476–482 (2004)
24. Schabmueller C.G.J., Koch M., Evans A.G.R., Brunnschweiler A.: *J. Micromech. Microeng.* **9**, 176–179 (1999)

**Authors' address:** Aharon Blank, Schulich Faculty of Chemistry, Technion–Israel Institute of Technology, Haifa 32000, Israel  
E-mail: ab359@tx.technion.ac.il